-):*(*;*ISSN: 2476-6909; Modares. Mech. Eng.

Modares Mechanical Engineering

DOI:

journal homepage: mme.modares.ac.ir

Design of a Hybrid Model Predictive Control for Control of Turbofan Engine

Mahboobeh Memari[1], Amir Esmaeili Abharian [2*], Alireza Izadbakhsh [3], Hasan Khalesi[4]

[1]Department of Electrical Engineering, Ga.C., Islamic Azad University, Garmsar, Iran

[2]Department of Electrical Engineering, Ga.C., Islamic Azad University, Garmsar, Iran

[3]Department of Electrical Engineering, Ga.C., Islamic Azad University, Garmsar, Iran

[4]Department of Electrical Engineering, Ga.C., Islamic Azad University, Garmsar, Iran

ARTICLE INFO

Article Type
Original Research

Article History
Received: **** **, *
Revised: **** **, *
Accepted: *** **, *
ePublished: **** **, *

ABSTRACT

The aero-engine control system plays the primary role in providing the requested thrust and monitoring the engine's critical parameters to prevent it from exceeding operational limits. Given that the engine parameters are changed following the new operational conditions and increased flight hours, obtaining a new model and then designing a new controller is needed, which causes switching in the model or controller. The most common control structures in the aviation field are gain-scheduled proportional-integral-derivative (PID) controllers and Min-Max algorithms or switching controllers. However, gain-scheduled PID controllers cannot cover the whole flight envelope. The Min-Max controllers are not guaranteed to prevent the limits from being exceeded exactly. Switching controllers can also generate unexpected outcomes because of abrupt changes in the time of the new controller. In this study a novel model predictive control is proposed based on a linearized model in the discrete-time domain for any operation point to solve the existing constraints. An adaptive algorithm based on a recursive least squares method matches the changes in engine dynamics. This new strategy ensures stable operation across various flight conditions. The required data are obtained from the gas turbine simulation program (GSP). Finally, the controller is simulated and evaluated via MATLAB/SIMULINK software. A comparison of our findings from the simulation with the available data revealed that the designed controller provides the needed fuel flow in all the power settings and satisfies all the considered constraints.

Keywords: Constrained adaptive Model Predictive Control (MPC), gas Turbine Engine, Fuel Flow Control, Recursive Least Squares (RLS), Gas Turbine Simulation Program

How to cite this article
Names, Title. Modares Mechanical Engineering; *(*): ****-****.

*Corresponding author's email: Aeabharian@srbiau.ac.ir
*Corresponding ORCID ID:0000-0003-0593-9773

Copyright© 2026, TMU Press. This open-access article is published under the terms of the Creative Commons Attribution-NonCommercial 4.0 International License which permits Share (copy and redistribute the material in any medium or format) and Adapt (remix, transform, and build upon the material) under the Attribution-NonCommercial terms.

Pre-Proof Version

شاپا: ۶۹۰۹-۲۴۷۶ مهندسی مکانیک مدرس. *؛*(*):*_*

مهندسی مکانیک مدرس

DOI:

صفحه اصلی مجله: mme.modares.ac.ir



طراحی کنترل‌کننده پیش‌بین مبتنی بر مدل ترکیبی به منظور کنترل موتور توربوفن

محبوبه معماری[۱]، امیر اسمعیلی ابهریان[۲*]، علیرضا ایزدبخش[۳]، حسن خالصی[۴]

[۱] گروه مهندسی برق، دانشگاه آزاد اسلامی، گرمسار، ایران
[۲] گروه مهندسی برق، دانشگاه آزاد اسلامی، گرمسار، ایران
[۳] گروه مهندسی برق، دانشگاه آزاد اسلامی، گرمسار، ایران
[۴] گروه مهندسی برق، دانشگاه آزاد اسلامی، گرمسار، ایران

اطلاعات مقاله

نوع مقاله
مقاله پژوهشی

تاریخچه مقاله
دریافت: **/**/****
بازنگری: **/**/****
پذیرش: **/**/****
ارائه آنلاین: **/**/****

چکیده

سیستم کنترل موتور هوایی نقش اصلی را در تأمین نیروی پیشرانش و پایش پارامترهای حیاتی ایفا می‌کند.تغییر پارامترهای موتور به دلیل تغییر شرایط عملیاتی و افزایش مداومت پروازی، محاسبه‌ی یک مدل جدید و طراحی یک کنترل کننده‌ی جدید را ضرورت می‌بخشد که این موضوع منجربه به بروز پدیده‌ی ناخوشایند سوییچینگ درکنترل کننده می‌شود. رایج‌ترین ساختار کنترلی مورد استفاده در صنعت هوایی، کنترل کننده‌های تناسبی- انتگرالی- مشتق‌گیر (PID) جدول بندی بهره، الگوریتم حداقل- حداکثر و کنترل کننده‌های سوییچینگ می‌باشند. کنترل کننده‌های PID جدول بندی بهره توانایی پوشش دهی کامل پاکت پروازی موتور نمی‌باشند. الگوریتم حداقل- حداکثر، نیز قادر به حفاظت پارامترها در زمان نزدیک شدن به محدودیت‌ها نمی‌باشد. کنترل‌کننده‌های سوییچینگ ممکن است اتفاقات غیرمنتظره‌ای را به دلیل تغییر ناگهانی از یک کنترل کننده به کنترل کننده‌ی دیگر در پی داشته باشند. در این مطالعه یک کنترل کننده‌ی پیش بین مبتنی بر مدل با ساختار جدید بر مبنای مدل خطی شده در حوزه‌ی زمان گسسته به ازای هر نقطه‌ی کار جدید پیشنهاد شده است. یک الگوریتم تطبیقی بر مبنای روش حداقل مربعات خطای بازگشتی دینامیک‌های متغیر موتور را تخمین می‌زند. داده‌های مورد نیاز در طول این تحقیق از نرم افزار شبیه سازی توربین گاز به دست آمده است. کنترل کننده با استفاده از نرم افزار متلب/سیمولینک شبیه سازی و ارزیابی می‌شود. در مقایسه‌ی بین یافته‌های حاصل از شبیه سازی با داده‌های آزمایشی در دسترس نشان می‌دهد که مقدار سوخت مورد نیاز در هر توان درخواستی با در نظر گرفتن تمام قیود موجود در سیستم، بطور مطلوب، توسط کنترل کننده‌ی طراحی شده تأمین می‌شود.

کلیدواژه‌ها: کنترل پیش بین تطبیقی مقید، موتور توربین گاز هوایی، کنترل میزان سوخت، حداقل مربعات خطای بازگشتی، برنامه شبیه سازی موتور توربین گاز

نحوه ارجاع به این مقاله
اسامی نویسندگان، عنوان مقاله، مهندسی مکانیک مدرس. * (*): ****-****.

*پست الکترونیکی نویسنده عهده‌دار مکاتبات: Aeabharian@srbiau.ac.ir
*شناسه ارکید نویسنده عهده‌دار مکاتبات: 0000-0003-0593-9773

Copyright© 2026, TMU Press. This open-access article is published under the terms of the Creative Commons Attribution-NonCommercial 4.0 International License which permits Share (copy and redistribute the material in any medium or format) and Adapt (remix, transform, and build upon the material) under the Attribution-NonCommercial terms.

In Press, Pre-Proof Version

In Press, Pre-Proof Version

1-Introduction

Owing to the increasing demand for high-performance aircraft with modern technologies in the aviation industry, either in civil or military areas, gas turbine engines (GTEs) or jet engines (GEs) have become the focus of attention as the power unit of the airplane [1]. Jet engine propulsion systems include a turbojet, a turboprop, and a turbofan. Their construction is single, twin, or triple spools [2]. Over time, aircraft engines have become more complex because of the increasing nonlinearities and need for special requirements in aero-engine functionality. Owing to the importance of the jet engine's proper response to various power settings in different maneuvers, the electronic control unit (ECU), as an advanced technology, plays a bold role in airplane performance[3].

A jet engine must have the best performance under varying environmental conditions and in various flight regimes such as take-off, idle, cruise, and acceleration/deceleration, with the protection of its operational and physical limitations. Some aero-engine physical and functional constraints are the turbine over-temperature, maximum shaft speed (over-speed), and compressor overpressure. The GE control system should ensure that the engine remains within its allowable operation range, independent of how the pilot applies the throttle. Additionally, a proper control system should be able to handle both control modes: power management and limit protection. The min-max multi-loop algorithm is usually used in the aero engine control system structures [4]. In this control structure, each variable under control has a separate regulator. Therefore, each controller produces a suitable fuel flow rate and simultaneously prevents the limits from exceeding. A shaft speed (Rotor) set-point is applied to the system as a pilot request representative. The generated fuel flow rate by the set-point controller, as the central controller is compared with each the minimum or maximum limit loop output. Finally, the min-max selector, the control input (fuel flow rate) that maintains all operational and safety limits, applies to the system. A limit protection controller includes a min-max structure that may be active even if it is not reaching its limit level. This conservative algorithm causes problems when a fast response is needed to obtain [5]. The main challenges in jet engine control systems include: 1. changing the GE dynamics for different reasons, such as the varying flight conditions and depreciation of components under long-term flight, and 2. finding a proper solution to protect the main parameters in the allowed range[6]. To solve the mentioned problems, an advanced control technique that incorporates system constraints into its optimization process must be considered. Because of the necessity of designing a proper control system for jet engines as the beating heart of this industry, comprehensive research has been conducted in this field [7]. PID control is one of the known controllers in the GE control structure. However, these controllers can cover only some operational points in the flight envelope. One is forced to use switching strategies to cover the whole operational area. In case of a sudden transfer from one controller/model to another in response to a change in engine dynamics, severe changes in the control signal occur, leading to dangerous events, including surges. Additionally, a min-max multi-loop algorithm is used in PID for limit protection. Still, this algorithm does not precisely guarantee the protection constraints and will be costly and complex (Fig. 1). As a result, alternative control strategies with simple architectures and similar or perhaps better performance are necessary.

Despite much research and work, no research has been presented in the open literature via the MPC approach for solving these problems simultaneously. In the current study, a novel adaptive model predictive control is used instead of the traditional controller, so there is no need to apply individual regulators for limit protection and a switching strategy for different flight conditions. For this purpose, at first, a recursive estimator (RLS) online estimates the model parameters, and then the constrained MPC control is developed so that the turbine exhaust temperature constraints are integrated into -the optimization process to generate control input. The available methods in nonlinear control systems are trial-and-error, feedback linearization, gain-scheduling, adaptive control strategy, and robust control. An adaptive control is a controller that can modify its behavior in response to system dynamics variations and disturbances. On the other hand, the adaptive control is a controller with tunable parameters and a mechanism for parameter tuning. Because of this tuning mechanism, the adaptive controller is nonlinear. The design process is as follows: a linearized model of the aero engine in the discrete state space form is first used to predict future outputs. The control effort is determined by optimizing a predefined cost function at every sample time. To solve the subject of the change in system dynamics due to the change in the operational conditions, an adaptive algorithm based on the identification method (described in detail in the following sections) is applied, which can manage the whole flight envelope. A jet engine has hybrid (algebraic and dynamic) equations, and the most well-known integration method for solving these equations is the Newton-Raphson algorithm based on iteration that, in turn, is challenging. A hybrid integration method (implicit and explicit integration method) is used to address this subject.

This study includes six sections. In Section 2, the challenges of designing the aero gas turbine engine control system are researched and investigated, emphasizing the necessity of using advanced control to meet high-performance and control requirements. This section also highlights the objectives and novelty of the research. A nonlinear dynamics model of the turbojet engine, by static and dynamic equations for each engine component, is presented in Section 3. Section 4 describes the control requirements and steps of the novel adaptive MPC control system design for jet engines. The simulation results and data analyses are given in Section 5. The findings are investigated and compared with the results of previous strategies in the discussion section.

2-Literature review

Due to the increasing use of gas turbine engines in the aviation industry to address engineering challenges in designing and constructing these systems, considerable research has been conducted. One of the best tools for research and investigation in this area, which, owing to safety and reduced cost, has particular importance, is nonlinear modeling and simulation of these systems. Regarding design time, construction, and engine tests, the modeling can be used in different forms. Despite many efforts in this area, achieving a more accurate model is necessary due to complex and nonlinear dynamics to improve current control systems.[7]. The control system is tested and verified on an exact model, can be implemented on a real engine, and prevents severe injuries due to improper control systems. In 2013, the authors developed a turbojet engine model in Simulink to obtain a safe flight regime in a transient mode with the desired surge margin[8]. Rahman and Whidborne modeled a turbojet engine via the volume dynamics method between components in Simulink, and they aimed to investigate the engine performance[9]. Martin et al., in a common study between industry and universities, developed an exact turbofan engine model with a control system in MATLAB Simulink[10, 11]. In 2024, Mykola Kulyk et al propose a review of mathematical models to investigate the gas flow path of the gas turbine engine[12]. This digital simulation was also the basis for many linear models that Pratt & Whitney applied to Systems Control, Inc., the controls research organization, for use in the LQR design procedure [13, 14]. A review of studies conducted in the field of aero-engine control revealed that many control strategies have been used to control the propulsion power of these engines [15-19]. In the early 21st century, the NASA Glenn Research Center proposed adaptive control strategies that apply the thrust estimated by the linear Kalman filter to generate the

In Press, Pre-Print Version

Thrust control directly[20].From 2005 to 2007, the authors reconstructed an advanced architecture called the full authority digital engine control (FADEC). They presented two different FADEC structures based on the thrust estimator [27-29]. What is certain is that all the above control methods require a Min-Max algorithm for limit protection to guarantee a safe and desired performance of aero-engines.

Despite advancements in control techniques, PID controllers are still commonly used in industrial processes, including aero-gas turbine engines. PID controllers are preferred because of their simple structure and robustness. The control of aero engines involves two modes: power management and limit protection (PID control, together with min-max control). However, the Min-Max architecture uses linear controllers to maintain constraints in the transient mode that can result in dangerous events if limit violations occur. This structure is a practical strategy to provide both control modes simultaneously[21]. Soheil Jafari et al. reported the results of the min-max strategy based on fuzzy T and S norms to improve the control system performance[22]. In [23], the authors tried to improve the Min-Max protection and decrease the existence of complex calculations in traditional Min-Max and Min-Max structures based on sliding mode control (SMC) methods using state feedback and optimization techniques. Aghasharifian Esfahani and Montazeri analyzed the application of the min-max algorithm in controlling turbofan engines. They used a genetic algorithm to identify min-max control parameters and reduce fuel consumption.

Another problem in jet engine control is wide-range operation, which requires different controllers in different flight conditions (altitude, Mach number). Also, one must provide proper performance in all operational ranges. For instance, one requires low fuel consumption for pending cruise flights and high power output as high as possible in the peak state[24]. Shuwei PANG et al. proposed a reduced model predictive control for thrust control of turbofan engines. Their study applied an adaptive MPC with online optimization to a turbojet engine as a case study.

In 2023, Q. Chen et al. proposed a subspace-based improved model predictive control (SIMPC) to manage hardness and solve the prediction model in predictive control. Then, an adaptive tuning method and a fuzzy logic tuner are presented[25]. In 2019, M. Montazeri-Gh et al. suggested the MPC control design with its hardware in the loop testing for control of the turbofan so that the controller model is linearized only at an operating point. In addition, the reference command is applied so that the performance of the control strategy is appraised around the desired operating point. This means that the proposed method cannot cover the entire flight envelope of engines and may need to be used in a switching manner[3]. In 2014, Liu Xiaofeng et al. presented a multi-loop control system and introduced the switching control theory[26].

A family of PID controllers is designed using the Min/Max switching method to prevent exceeding limits. Y. Shi and X.-M., in 2021, proposed a bump-less transfer control method to address the switching problem that prevents the discontinuity of the control input while maintaining the stability of the system[27]. The method proposed by Y. Shi and X.-M involves an unconstrained controller, and the protection of limits is one of the critical issues in the design process. In[28], the authors proposed an innovative method to address the switching problem in complicated systems. Wenhao XU et al., 2020 presented a new limit protection method for constraint management of a turbofan engine [29]. They proposed an add-on control scheme based on the closed-loop model called the linear parameter varying (LPV) to prevent exceeding the permissible limit. The proposed method in this study can manage all constraints via quadratic programming integrated into a simple predictive controller. Authors in [30] investigated and managed the nonlinear dynamics of system in presence of physical constraints by nonlinear model predictive control. The literature review indicates that much research is dedicated to modeling and gas turbine aero engines. Much research has been done to increase the accuracy of the modeling, but achieving real-time simulation is a significant challenge. This limitation prevents the development of advanced control systems that can manage the performance of aero engines in actual maneuvers. In addition, existing control strategies such as PID control, min-max algorithms, and switching controllers have limitations. PID controllers must use a gain schedule for any particular range to cover the whole operation envelope or apply PID control for any operation range. In contrast, Min-Max controllers do not have enough accuracy for limit protection. On the other hand, switching controllers can cause unexpected events due to abrupt changes in the time of controller exchange. Furthermore, many control strategies are based on learning algorithms or adaptive control methods that require vast experimental data, complicated structures, and implementation limitations.

To date, no open research has been presented on turbojet engine controller design; however, while keeping the control strategy simple and using dynamic modeling, the controller can cover all flight points in addition to real-time implementation.

The innovation of this research lies in introducing a constrained adaptive MPC controller. This control strategy proposes a novel, simple method for designing an advanced controller to solve the challenge of the turbojet engine control system. This study's introduction of adaptive MPC represents an implementation manner for controlling turbojet engine performance under constraints in various flight conditions. An adaptive method based on identification via the RLS technique is proposed to address the challenge of changing flight conditions and switching control theory in aircraft engines. Indeed, there is no need for a new model or coefficient for the controller; using the identification, a new internal model for the MPC controller is identified, the coefficient controller is computed, and finally, the required controller command, the fuel flow rate, is calculated. This way, we can control the engine's dynamics at all power settings and cover the entire flight envelope.

The best performance is usually obtained near the engine's variable limits. However, exceeding these limits can cause dangerous events such as surge phenomena or damage to engine components.

Therefore, the protection problem in the engine control system is a critical subject. Instead of using conservative structures such as the min-max controller, an advanced controller that can predict before arriving at these limits, called the constrained MPC controller, is presented. In this method, constraints are integrated into the Hildreth technique,and after the cost function is optimized, a proper control command for every new flight condition is obtained.

In Press, Pre-Proof Version

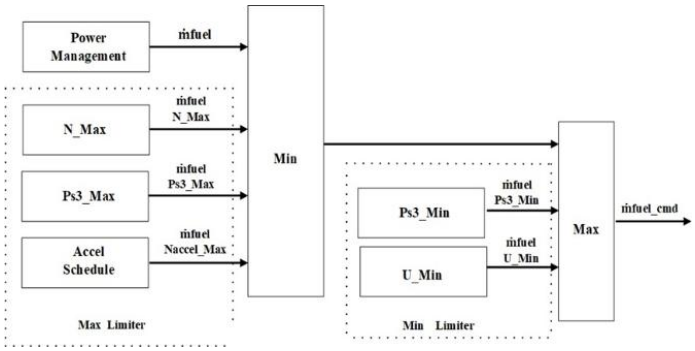

Figure 1- Multi-loop control with min-max structure for power management and limit protection in aero-engine control system [8].

In Press, Pre-Proof Version

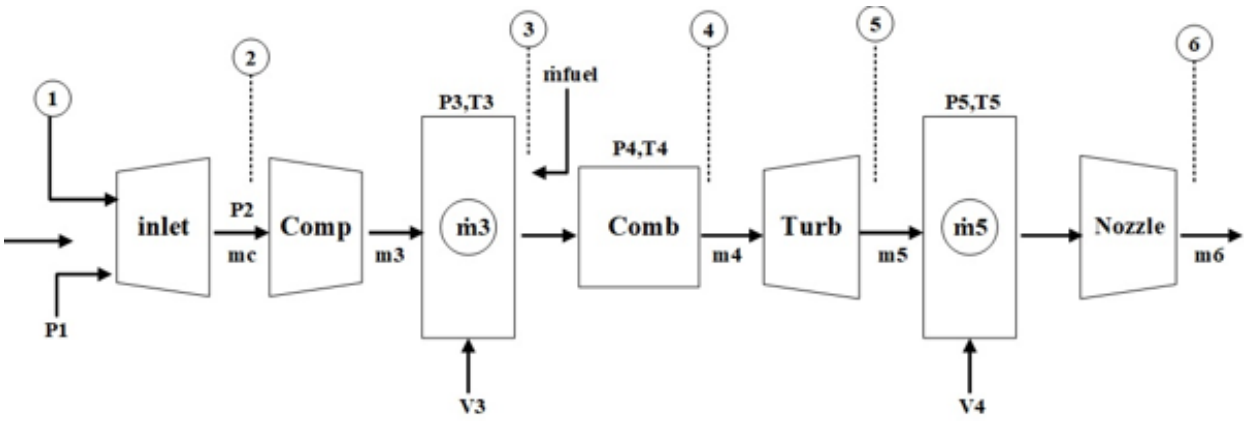

Figure 2- Single-spool turbojet engine dynamic model station numbering with inter-component volumes [10].

3-The engine thermodynamic model

This study investigated a single-spool turbojet engine. The engine components are shown in Fig. 2. The operation of the thermodynamic model, such as steady-state and transient, was evaluated via the Gasturb10 software. The required features of the turbojet under study are reported in Table 1. In this work, each component is modeled individually, called the component level model (CLM), based on the thermodynamic relationship in the inlet, compressor, combustor, turbine, and nozzles, together with the characteristic map. Each map includes several lookup tables based on the relationship between the element's efficiency, pressure ratio, and corrected mass flow, which are functions of the corrected rotor speed and β-lines. In the following subsections, the performance of each component is discussed in detail.

3-1-Inlet

The intake diffuser brings free air into the engine and only guides the flow to the compressor. It means that the inlet does not do any work on the flow. However, the pressure recovery of the free stream affects the performance of the inlet. Also, in this section, the engine is assumed to be an isentropic process for airflow. Additionally, the heat transfer and friction of the flow with the inlet walls and the dynamic behavior of air are neglected.

3-2-Compressor

The air conditions that enter the engine from the intake up to the compressor are defined based on the Mach number and inlet efficiency**[31]**. The inlet total temperature and pressure of the compressor are equal to [12, 26, 27]:

$$\boldsymbol{T_2 = T_{Amb}\left(1+\left(\frac{\gamma-1}{2}\right)M^2\right)} \quad (1)$$

$$\begin{cases} P_2 = P_{Amb}\left(1+\eta_l\left(\frac{\gamma-1}{2}\right)M^2\right)^{\frac{\gamma}{\gamma-1}} & if\ M<1 \\ P_2 = P_{Amb}\left(1+\left(\frac{\gamma-1}{2}\right)M^2\right)^{\frac{\gamma}{\gamma-1}} \times (1-0.075\times(M-1)^{1.35}) & if\ M>1 \end{cases}$$

$$\gamma = \frac{C_P}{C_P - R} \quad (2)$$

The compressor is modeled as a single block in Simulink, and the stages' dynamic behavior is also considered a single block using the compressor's inlet and exit conditions. A characteristic map is utilized to determine the compressor's steady-state behavior. The gas dynamics in the compressor are computed by applying thermodynamic equations such as the continuity, power, and ideal gas equations to the considered volume between the compressor and the combustor.

The mathematical equations and continuity equations are used to model the inter-component volume for the compressor in Simulink. The reader referred to **[2, 32]** for details. The compressor parameters are defined by the following expressions **[33]**:

$$\boldsymbol{N_{c,Co} = \frac{N_{rotor}}{N_{rotor_des}\sqrt{\frac{T_2}{T_{2des}}}}} \quad (3)$$

$$\boldsymbol{\dot{m}_{c,Co} = f_1(\beta, N_{rotor_c,Co})} \quad (4)$$

$$\boldsymbol{\eta_{Co} = g_1(\beta, N_{rotor_c,Co})} \quad (5)$$

$$\boldsymbol{T_3 = T_2\left\{1+\frac{1}{\eta_{Co}}\left(\left(\frac{P_3}{P_2}\right)^{\frac{\gamma-1}{\gamma}}-1\right)\right\}} \quad (6)$$

The work done by the compressor is calculated from the expression.

$$pw_{Co} = \dot{m}_{3out} \times C_p \times (T_3 - T_2) \quad (7)$$

As mentioned, the gas dynamics in the compressor are derived by applying the thermodynamic equations to the inter-component volume between the compressor and the combustor:

$$\frac{d}{dt}W_3 = \dot{m}_{3in} - \dot{m}_{3out} \quad (8)$$

$$\frac{d}{dt}(T_3) = \frac{1}{W_3 C_v}\{[\dot{m}_{3in} \times (C_p T_{3in} - C_v T_{3out})] - [\dot{m}_{3out} \times R \times T_3]\} \quad (9)$$

$$\boldsymbol{P_3 = \frac{W_3 \times R \times T_3}{V_3}} \quad (10)$$

3-3-Combustor

Here, it is assumed that the combustion process performs instantaneously and wholly after the fuel is provided to the combustor

In Press, Pre-Proof Version

[1]. In the actual process, a pressure drop occurs during combustion, and the pressures at the input and exit of the chamber are not equal.

Table 1- Design point specifications of the studied turbojet engine

Number	Specification	Value
1	Inlet mass flow (kg/s)	19.9
2	Diffuser pressure ratio	1
3	Shaft speed (rpm)	16540
4	Compressor pressure ratio	6.920
5	Compressor efficiency	0.825
6	Combustor-chamber efficiency	0.985
7	Combustor chamber pressure loss percent	0.04%
8	Fuel type	JET-A
9	The calorific value of fuel (kJ/kg)	430031
10	Turbine pressure ratio	2.5017
11	Turbine efficiency	0.88
12	Nozzle throat area (m^2)	0.060
13	Inlet mass flow (kg/s)	19.9

Therefore, it causes the gases to flow in the correct direction, and the combustor mass flow rate is calculated. The pressure drop, across the combustor is calculated by

$$\Delta P = \dot{m}_{4in} = \sqrt{\frac{P_3 - P_4}{P_{cal}}} \quad (11)$$

Where,P_{cal}, the pressure loss coefficient of the combustor, which is at different speeds. The combustor modeling as a single one-dimensional volume is also done in Simulink using thermodynamic equations and algebraic equations for the pressure drop in the combustor.

$$\frac{d}{dt}W_4 = \dot{m}_{4in} - \dot{m}_{4out} + \dot{m}_{fuel} \quad (12)$$

$$\frac{d}{dt}T_4 = \frac{1}{W_4 C_{v4}}\left[\left((LHV.\eta_{ch} - C_{v4}T_4).\dot{m}_{fuel}\right) \times (\dot{m}_4.R.T_4) + \left(\dot{m}_3 \times (C_{p4}.T_b - C_{v4}T_4)\right)\right] \quad (13)$$

$$P_4 = P_3 - \Delta P \quad (14)$$

Where,LHV and V_4 are the lower calorific value (kJ/kg) and control volume value (m^3), respectively. In eq.13,T_b is the combustor interpolation constant is equal to:

$$T_b = \beta_b \times T_3 + (1 - \beta_b) \times T_4 \quad (15)$$

The combustor-specific heats are obtained at the interpolated temperature of the combustor.

3-4-Turbine

Like the compressor, the turbine, and the dynamic behavior of the turbine stages are also modeled with a single block in Simulink according to the turbine's inlet and exit conditions. The turbine characteristic map is also similar to the compressor performance curve based on β lines in the form of lookup tables (Fig.4). Efficiency and the corrected mass flow rate are functions of β, the corrected rotor speed, and the outlet temperature of the turbine are expressed below.

$$\eta_{tur} = g_2(\beta, N_{rotor_c,tur}) \quad (16)$$

$$\dot{m}_{c,5} = f_2(\beta, N_{rotor_c,tur}) \quad (17)$$

$$\beta = \frac{pr - pr_{min}}{pr_{max} - pr_{min}} \quad (18)$$

$$T_5 = T_4\left(1 + \eta_{tur}\left[\left(\frac{P_5}{P_4}\right)^{\frac{\gamma-1}{\gamma}} - 1\right]\right) \quad (19)$$

Where the steady-state performance of the components is described by turbine maps that are shown by $g_2, f_2$and are performed by using look-up tables in Simulink. The β-lines are hypothetical lines and have no physical meaning and pr describes the pressure ratio.
The work done on the turbine can be calculated from the following equation:

$$Pw_{tur} = \dot{m}_{5out} \times C_{p4} \times (T_5 - T_4) \quad (20)$$

The turbine is also modeled as a mixing volume in the transient process. The gas dynamics are also obtained using the thermodynamic equations for the considered volume between the turbine and the convergent nozzle.

$$\frac{d}{dt}W_5 = \dot{m}_{5in} - \dot{m}_{5out} + Bld \quad (21)$$

$$\frac{d}{dt}T_5 = \frac{1}{W_5 C_{v4}}\left[\left(\dot{m}_{5in} \times (C_{p4}.T_{5in} - C_{v4}T_{5out}\right) - (\dot{m}_{5out} \times R \times T_5)\right] \quad (22)$$

$$P_5 = \frac{W_5 \times R \times T_5}{V_5} \quad (23)$$

3-5-Nozzle

The studied turbojet has a convergent nozzle. The nozzle's airflow is assumed to be quasi-steady state, so the nozzle dynamics are neglected. The nozzle mass flow rate is defined based on the nozzle back pressure, P_{back} and the nozzle exit critical pressure (P_{cr}). A nozzle critical back pressure for a specific inlet pressure is equal to:

In Press, Pre-Proof Version

$$P_{cr} = \left(\frac{2}{1+\gamma_b}\right)^{\frac{\gamma_b}{\gamma_b - 1}} P_{inlet} \quad (24)$$

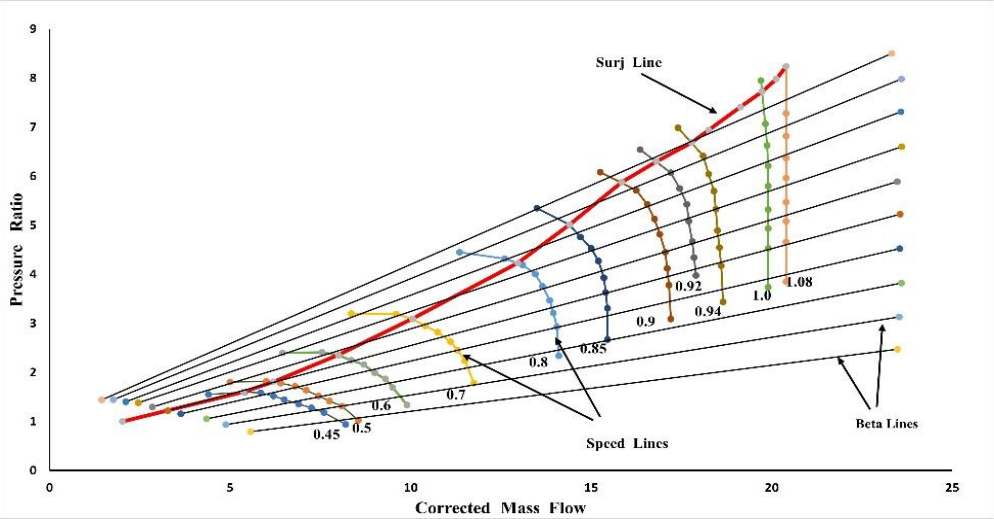

Figure 3- Compressor performance curve (compressor pressure ratio vs corrected mass flow) with β-lines that are extracted from GSP.

According to the critical pressure, the nozzle mass flow rate will be calculated below.

$1 - \ if \ P_b > P_{cr}$

$$\begin{cases} P_e = P_b \\ \dot{m}_6 = \frac{P_5}{\sqrt{RT_5}} A_N \left(\frac{P_e}{P_5}\right)^{\frac{1}{\gamma_b}} \sqrt{\frac{2\gamma_b}{\gamma_b - 1}\left[1 - \left(\frac{P_e}{P_5}\right)^{\frac{\gamma_b - 1}{\gamma_b}}\right]} \end{cases} \quad (25)$$

$2 - \ if \ P_b < P_{cr}$

$$\begin{cases} P_e = P_{cr} \\ \dot{m}_5 = \frac{P_5}{\sqrt{RT_5}} A_N \sqrt{\gamma_b \left[1 - \left(\frac{2}{\gamma_b + 1}\right)^{\frac{\gamma_b + 1}{\gamma_b - 1}}\right]} \end{cases} \quad (26)$$

Where, $\boldsymbol{A_N}$, $\boldsymbol{P_e}$, $\boldsymbol{\dot{m}_6}$ and $\boldsymbol{\gamma_b}$, are the nozzle throat area ($\boldsymbol{m^2}$), nozzle exit pressure (psi), nozzle mass flow rate, and the specific heat ratio, respectively.

3-6-Shaft dynamics

The assumption is that a turbojet engine that has a single spool is working in a steady state. The control system suddenly reduces fuel flow, reducing the temperature of combustion products and turbine output power. This power is less than the power needed for the compressor, so an unbalanced power is produced in the transient mode [34].

$$\frac{dPw}{dt} = Pw_{tur} - Pw_{Co} \quad (27)$$

This unbalanced power then causes inverse acceleration in the spool. The changing procedure is as follows:

$$\dot{N}_{rotor} = \left(\frac{60}{2\pi}\right)^2 \cdot \frac{1}{I.N_{rotor}} \cdot \frac{dPw}{dt} \quad (28)$$

Therefore, I, pw_{tur}, $and\ pw_{Co}$ are the shaft moment of inertia, and the turbine and the compressor work respectively.

4-A novel aero-engine fuel control system design

As mentioned before, achieving the best response to the pilot's requested thrust and protecting the critical variables from exceeding their limits is the main task of the aero-engine control system. However, engine dynamics (time-variant variables) notably vary with changing flight conditions. The first step in designing a model-based control system for a jet engine is to obtain a proper model for every operating point. Instead of model linearization at every new operating point, determining a new model, and controller re-tuning or redesigning, it is necessary to use an adaptive controller with an estimator based on the specified structure (ARX). The estimator uses one of the standard estimation methods called least squares error (LS), then using the past outputs and control input, the new system dynamics are estimated online, and the controller coefficient is self-tuned to fit new operating conditions. The predictive control along the optimization process also integrates the constraints of system parameters and then generates control input in each operating condition.

This process repeats at each sample time. The recursive estimation method (Recursive Least Squares) reduces the computational burden in the estimation process. The system dynamics vary more slowly than parameter adaptation, and according to the online recursive estimation, this controller can be used in real applications. To investigate whether that proposed controller is feasible, the hardware in the loop is a future work. To verify the identified model, the

In Press, Pre-Proof Version

calculated output by the engine nonlinear equations should be compared with the identified output by the RLS method. As shown in Fig. °, the identified output with a 0.023% error matches the nonlinear dynamic model output. The convergence error of one of

the estimated parameters via the RLS is shown in Figure 6. The gas temperature in the burner exit must be maintained within the allowable limit to prevent turbine physical damage and thus increase the engine's life. Due to the high gas temperature of this section of

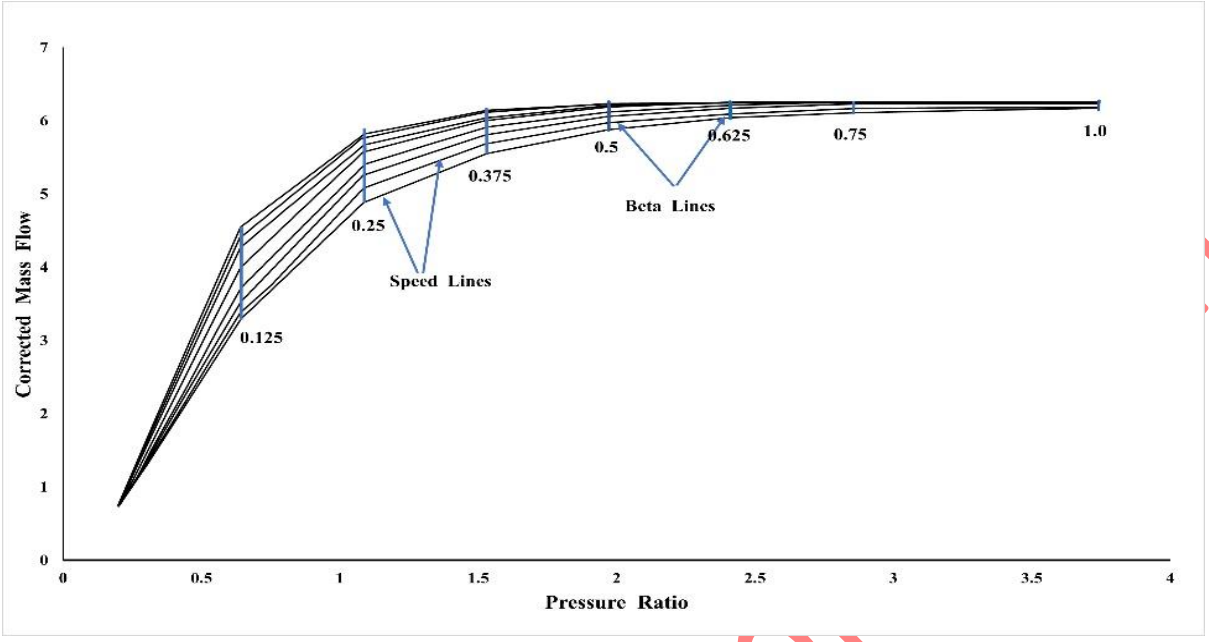

Figure 4- Turbine performance curve (corrected mass flow vs turbine pressure ratio) with β-lines that are extracted from GSP

-the engine, it is very high and difficult or even impossible to measure; therefore, the turbine outlet temperature. T_5, is considered. Also, the airflow stagnation causes airflow loss and results in a high primary burner fuel/air ratio. Therefore, the turbine inlet temperature may increase. The engine control system should be able to provide over-temperature protection. With respect, the air/fuel ratio is different among the various engines (the ratio of air to fuel with a considered pressure must be within the proper range to perform a good combustion), the amount of injected fuel in the burner is essential, which may cause the burner to blow out (flame out) [41]. These disadvantageous factors limit engine operation. These constraints can be managed by controlling the main parameters. The maximum limit of the turbine temperature $(T_5)_{max}$ is considered to prevent the engine from hot start in the ground start process and to protect the engine.

In Table4, the bound values of the parameters are reported. A constrained MPC controller designed to compute the fuel flow rate as the control input while maintaining variables, such as T_5 under the maximum limit level.

4-1-Indirect adaptive algorithm

The jet engine dynamics change due to the ambient temperature and pressure variations under various operational conditions (Mach and flight altitude). They try to create uncertainty in the engine parameters. A suitable control system should maintain the engine operation at the highest level and stabilize the system throughout the flight envelope. Because of the simplicity and feasibility of linear controllers, they are commonly used in aero-engine control systems**.** Available nonlinear control design methods include trial-and-error, linearization, robust control, adaptive control, and gain scheduling. The linearization is only valid within a neighborhood of approximately 3-5% of that operating point; therefore, it cannot control an aero-engine in all operation points. One solution to the challenges of nonlinearities outside the linearization range is dividing the operating range into many operating points and then using the piecewise linearization method. In [31], the gain scheduling controllers as a class of adaptive controllers in the jet

-engine control system are investigated.

Due to the offline adaptation method, uncertainties have arisen in various environmental conditions that these controllers cannot consider. Because of the lack of accurate gain tuning, dangerous circumstances such as system instability may occur. In the linear model-based control structure, it is necessary to have a suitable linear model for every operating point. Still, the switching method needs to be used to cover the entire flight envelope. This study has researched and investigated the model uncertainties due to the variation in operating conditions and nonlinearities resulting from linearization at different operating points. To address the challenges raised, instead of dividing the operating range into a high number of operating points and then the piecewise linearization to deal with the difficulties of nonlinearities outside the linearization range, an adaptive technique, including a recursive online estimator called adaptive self-tuning control, has been used. Although a robust control technique is also practical for designing a nonlinear control system with appropriate robustness, adaptive control is superior for controlling systems with slowly changing parameters. The main reason for this is the learning behavior of the adaptive controller. Adaptive control improves its performance during adaptation, while robust control tries to maintain its adaptive performance.

Furthermore, adaptive control requires little or no information about prior estimates. In contrast, a robust controller requires reasonable prior estimates within the parameter range, which is challenging in real-time applications. In adaptive control, unknown engine parameters are estimated online and recursively based on past measured inputs and outputs. Therefore, the model is identified

In Press, Pre-Proof

online and at any moment per new operating conditions and is used as the internal predictive control model.
In this way, using the RLS method as an estimation or adaptation mechanism reduces the uncertainty of the system parameters, prevents instability due to model inaccuracy, and increases system robustness. Due to the recursive nature of the estimation process and the controller's lack of prior estimates, there is no need to store estimations. Therefore, the dimensions of the data matrix and the computational burden is reduced.

Table 2- MPC controller coefficients

Number	Controller coefficients	value
1	r_w (adjustment parameter for the closed loop desired performance)	30000
2	N_p (predictive horizon)	60
3	N_C(control horizon)	30
4	T_s (sample time, sec)	0.0025

In addition, Hildreth's quadratic programming algorithm (explained in the following) makes this controller suitable for real-time applications[35].

4-1-1-Recursive methods of least squares (RLS)

Consider the transfer function of a deterministic linear model in the discrete domain as the internal model of the MPC controller at every operating point individually, as follows:

$$G_p(z) = \frac{y_u(z)}{u(z)} = \frac{B(z^{-1})}{A(z^{-1})} = \frac{\beta_0+\beta_1 z^{-1}+\cdots+\beta_l z^{-l}}{1+\alpha_1 z^{-1}+\cdots+\alpha_l z^{-l}} \quad (29)$$

So that, $\alpha_1, \alpha_2, \dots, \alpha_l$ and $\beta_1, \beta_2, \dots, \beta_l$ are the model parameters. Therefore, the difference equation of eq. (29) in the time domain is equal to:

$$y_u(k) + \alpha_1 y_u(k-1) + \cdots + \alpha_l y_u(k-l) = \beta_1 u(k-1) - \cdots - \beta_l u(k-l) \quad (30)$$

By putting the measured values, $y(k)$, rather than the model output $y_u(k)$, and the estimated parameters into the above expression, the prediction equation of the output, $y(k)$ according to the measurements up to $k-1$ are indicated in the following form.

$$\hat{y}(k|k-1) = -\hat{\alpha}_1(k-1)y(k-1) - \cdots - \hat{\alpha}_l(k-1)\, y(k-l) + \hat{\beta}_1(k-1)u(k-1) + \cdots + \hat{\beta}_l(k-1)u\big(k = \psi^T(k)\hat{\theta}(k-1) - l\big) \quad (31)$$

The data vector is obtained as follows:

$$\psi^T(k) = \big(-y(k-1) \dots - y(k-l)\big|u(k-1) \dots u(k-l)\big) \quad (32)$$

The parameter vector is equal to:

$$\hat{\sigma}^T(k) = \big(\hat{\alpha}_1 \dots \hat{\alpha}_l\big|\hat{\beta}_1 \dots \hat{\beta}_l\big) \quad (33)$$

Now, the equation error can be interpreted as

$$\mathrm{E}(k) = y(k) - \hat{y}(k|k-1) \quad (34)$$

Where, $y(k)$, and $\hat{y}(k|k-1)$ are the new observations and the one-step prediction of the model output, respectively.

$$(k) = \psi^T(k)\hat{\sigma}(k-1) + E(k) \quad (35)$$

$N+1$, equations are written in matrix form as:

$$y(l+N) = \psi(l+N)\hat{\sigma}(l+N-1) + E(l+N) \quad (36)$$

Thus, that

$$y^T(l+N) = \big(y(l)\, y(l+1) \dots\ y(l+N)\big) \quad (37)$$

And, the data matrix

$$\psi(l+N) = \left(\begin{array}{ccc|ccc} -y(l-1) & \cdots & -y(0) & u(l-1) & \cdots & u(0) \\ -y(l) & \cdots & -y(1) & u(l) & \cdots & u(1) \\ \vdots & & \vdots & \vdots & & \vdots \\ -y(l+N-1) & \dots & -y(N) & u(l+N-1) & \cdots & u(N) \end{array}\right) \quad (38)$$

The cost function is considered in the LS method in the form below.

$$V = E^T(l+N)E(l+N) = \sum_{k=l}^{l+N} E^2(k) \quad (39)$$

And,

$$E^T(l+N) = \big(E(l)E(l+1) \dots E(l+N)\big) \quad (40)$$

Therefore, the non-recursive parameter estimation vector is

$$\hat{\sigma} = (\Psi^T\Psi)^{-1}\Psi^T y \quad (41)$$

Owing to the LS method being implemented offline, the estimation of the parameters is only available after the end of the measurement. The matrix Ψ has the dimension $(\boldsymbol{N+1}) \times \boldsymbol{2l}$, and therefore, it gets too large for a long-term measurement period. Recursive methods are more suitable for aero-engines for several reasons: they decrease the computation burden, provide the new estimation after each step, and do not need to save a priori-measurements; therefore, they are more suitable for real-time applications. The parameter estimation by the RLS algorithm for the step (k+1) is calculated by:

$$\hat{\sigma}(k+1) = \hat{\sigma}(k) + \mu(k)(y(k+1) - \psi^T(k+1)\hat{\sigma}(k)) \quad (42)$$

Where $\mu(k)$ is the correction vector in the form below.

$$\mu(k) = M(k+1)\psi(k+1) = \frac{1}{\psi^T(k+1)M(k)\psi(k+1)+1} M(k)\psi(k+1) \quad (43)$$

In Press, Pre-Proof Version

To obtain the equations and explanations in detail, refer to the Appendix. A and reference [36]. The state-space matrices of the identified linear model by the RLS method at the design point (Mach=0 and altitude 0 (m)) are as follows:

$$A_1=\begin{bmatrix}1.14 & 1 & 0 & 0 & 0\\ -0.08269 & 0 & 1 & 0 & 0\\ -0.04943 & 0 & 0 & 1 & 0\\ -0.07732 & 0 & 0 & 0 & 1\\ 0.03399 & 0 & 0 & 0 & 0\end{bmatrix} \qquad B_1=\begin{bmatrix}1.804\\ 0.6713\\ 0.006675\\ -0.01191\\ 0\end{bmatrix}$$

$$C_1=[1 \quad 0 \quad 0 \quad 0 \quad 0] \qquad D_1=0$$

(44)

The PID coefficients are a function of the environmental conditions, which are depicted as the lookup table form called gain schedule to cover the whole of the flight envelope.

4-2-Model predictive control

The overall purpose of the predictive controller is to calculate the control input for the optimization of the future behavior of the system output. Optimization is conducted via the previous inputs and outputs of the system during a finite time window (control horizon). The obtained linear model in the last section is transformed to the state space form below:

$$x(k+1)=A_1x(k)+B_1u(k)$$

$$y(k)=C_1x(k)+D_1u(k)$$

(45)

Where,$x(k)=[N_{rotor} \quad T_5]^T$, is the system state vector, including the rotor speed N_{rotor} (rpm) and turbine exhaust temperature (T_5). The fuel flow rate,$\dot{m}_f$ is only the input variable $u(k)$ and the rotor speed,N_{rotor} is the system output. $\left(y(k)=[1 \quad 0]\begin{bmatrix}N_{rotor}\\ T_5\end{bmatrix}\right)$.

To satisfy the design aim, attain offset-free set-point tracking, and attenuate disturbance effects, an integrator is considered within the model; in this case, the model is called the augmented model [35]. It is presumed that the output $y(k)$ is not affected by the control input $u(k)$ simultaneously means that D = 0 in the model. The control increment input is in the form:

$$\Delta u(k)=u(k)-u(k-1) \tag{46}$$

Then, a new state vector is selected in the following form:

$$x_a(k)=[\Delta x(k)^T y(k)]^T \tag{47}$$

So that $\Delta x(k)=x(k)-x(k-1)$ and the new discrete state-space equations (the augmented model) are as follows:

$$\underbrace{\begin{bmatrix}\Delta x(k+1)\\ y(k+1)\end{bmatrix}}_{x_a(k+1)}=\underbrace{\begin{bmatrix}A & 0^T\\ CA & I\end{bmatrix}}_{A_a}\underbrace{\begin{bmatrix}\Delta x(k)\\ y(k)\end{bmatrix}}_{x_a(k)}+\underbrace{\begin{bmatrix}B\\ CB\end{bmatrix}}_{B_a}\Delta u(k) \tag{48}$$

$$x_a(k+1)=A_ax_a(k)+B_a\Delta u(k)$$

$$y_a(k)=C_ax_a(k)$$

(49)

Where $\underline{0}=[0\,0\cdots 0]$ is zero vector with dimension (n) and the model used in the design of the controller is the augmented model (A_a,B_a,C_a). Suppose the state variables are available up to sampling moment (k). The predicted outputs (concerning) the current information of the state variable $x(k)$ and futurity path $\Delta u(k+j|k)$ are equal to:

$$\Delta U_k = [\Delta u(k|k)\ \Delta u(k+1|k)\ \Delta u(k+2|k)\ \dots \Delta u(k+j-1|k)]$$

for $j=0,1,\dots,N_c$

(50)

Y=
$[y(k+1|k)\ y(k+2|k)\ y(k+3|k)\ \cdots y(k+i|k)\ ]^T$

for $i=0,1,\cdots,N_p$

(51)

The predicted outputs in matrix form are rewritten as

$$Y=Fx_a(k_i)+\varphi\Delta U \tag{52}$$

So that

$$F=\begin{bmatrix}C_aA_a\\ C_aA_a{}^2\\ C_aA_a{}^3\\ \vdots\\ C_aA_a{}^{N_p}\end{bmatrix} \tag{53}$$

$$\varphi=\begin{pmatrix}C_aB_a & 0 & 0 & \cdots & 0\\ C_aA_aB_a & C_aB_a & 0 & \dots & 0\\ C_aA_a{}^2B_a & C_aA_aB_a & C_aB_a & \cdots & 0\\ \vdots & \vdots & \vdots & \dots & \vdots\\ C_aA_a{}^{N_p-1}B_a & C_aA_a{}^{N_p-2}B_a & C_aA_a{}^{N_p-3}B_a & \dots & C_aA_a{}^{N_p-N_c}B_a\end{pmatrix}$$

(54)

The index function J is defined as follows:

$$J=\sum_{i=0}^{N_p}(R_s-Y)^T(R_s-Y)+\sum_{j=0}^{N_c-1}\Delta U^T\bar{R}\Delta U \tag{55}$$

Where,

$$\bar{R}=r_wI_{N_c\times N_c} \tag{56}$$

$$R_s=\bar{R}_sr(k_i) \tag{57}$$

$$\bar{R}_s=\overbrace{[1\ 1\ 1\ \cdots 1]^T}^{N_p} \tag{58}$$

r_w,$r(k_i),N_p$, are the tuning coefficient, input signal at k_i, moment, and the predictive horizon, respectively. The goal of controller design is to obtain the best command vector ΔU to

In Press, Pre-Proof Version

reduce the difference between the reference input and the predicted output.

To find the optimal control input vector to minimize the cost function, eq. (52) should be used as follows:

$$J = (R_S - Fx_a(k_i))^T(R_S - Fx_a(k_i)) - 2\Delta U^T\varphi^T(R_S - Fx_a(k_i)) + \Delta U^T(\varphi^T\varphi + \overline{R})\Delta U \quad (59)$$

Therefore, the control signal (fuel flow rate) for the unconstrained system (aero-engine) will be obtained in the following form:

$$\Delta U = (\varphi^T\varphi + \bar{R})^{-1}\varphi^T(R_s - Fx_a(k_i)) \quad (60)$$

Where $(\varphi^T\varphi + \bar{R})$ is a positive definite matrix, but during fast sampling of dynamics in complex systems or systems with closed-loop high performance, the desired evaluation of the control increment signal Δu may cause poor numerical solutions and heavy computational load during online implementation. In designing the MPC, using the Laguerre is a more suitable resolution.

4-2-2-Constrained model predictive control

Due to structural limitations of the engine components and various restrictions in the control commands applied to the actuators, the controller designed in the previous sections cannot control the aero engine safely. To address this problem, a predictive control problem in the presence of limits will be formulated via the quadratic programming method called the Hildreth quadratic programming method.

4-2-2-1-The Hildreth quadratic programming method

Consider the constrained performance index as follows:

$$J = \frac{1}{2}\Delta U^T Z\Delta U + \Delta U^T f \quad (61)$$

So that

$$Z = (\varphi^T\varphi + \bar{R})^{-1} \quad (62)$$

$$f = (\varphi^T R_s - \varphi^T Fx_a(k_i)) \quad (63)$$

Linear inequality constraints are formed as follows:

$$A_{cons}\Delta U \le b \quad (64)$$

Where, A_{cons} indicates the constraints matrices based on the incremental control input, so that

$$A_{cons=}\begin{bmatrix} I \\ I \end{bmatrix} \quad (65)$$

$$b = \begin{bmatrix} u_{max} - u(k-1) \\ B^{-1}((x_{max} - x(k)) - A\Delta x(k)) \end{bmatrix} \quad (66)$$

Finally, by taking the derivative of the constrained performance index (eq.61) and calculating Lagrange coefficients as follows:

$$\lambda_i{}^{m+1} = max(0, w_i{}^{m+1}) \quad (67)$$

$$w_i{}^{m+1} = -\frac{1}{h_{ij}}\left[k_i + \sum_{j=1}^{i-1} d_{ij}\lambda_j{}^{m+1} + \sum_{j=i+1}^{n} d_{ij}\lambda_j{}^{m}\right] \quad (68)$$

$$d = A_{cons}Z^{-1}A_{cons}{}^T \quad (69)$$

$$K = b + A_{cons}Z^{-1}f \quad (70)$$

So that (d_{ij}), is the $ij-th$ component in the d matrix, and k_i, is the $i-th$ component in vector (K). Note that λ is a vector that includes Lagrange coefficients, and all of the elements in this vector are equal to zero or positive.

The constrained MPC control low (fuel flow rate) for the aero-engine is generated as follows:

$$\Delta U = (-Z^{-1}f) - (Z^{-1}A_{cons}{}^T\lambda) \quad (71)$$

All system constraints, such as the control input and state variables, are applied to the controller (Hildreth quadratic programming) as parameter b in equation (71). For more details, refer to [35]. It is remembered that only the maximum values are considered for constraints here.

5-Results

A single-spool turbojet engine that can produce 3500lbf (16KN) thrust is considered a case study. In Table ١, the turbojet engine design point specifications are described. These parameters are similar to the turbojet engine specifications accessed by the gas turbine simulation program (GSP). As mentioned earlier, the adaptive algorithm estimates the model parameters in each new operating point. A thermodynamic component level model using the equations of Section 4 and GSP data is implemented in the MATLAB-SIMULINK environment as the nonlinear plant. This nonlinear model includes characteristic curves (maps) of the engine rotary components so that its requirement data (constants, design point parameters, maps) is obtained from the GSP software. The compressor and turbine maps are shown in Figs. (3) and Fig. (4), respectively. In the compressor map, the pressure ratio lines vs air mass flow, are vertical at very high speeds and horizontal at very low speeds.

In Press, Pre-Proof Version

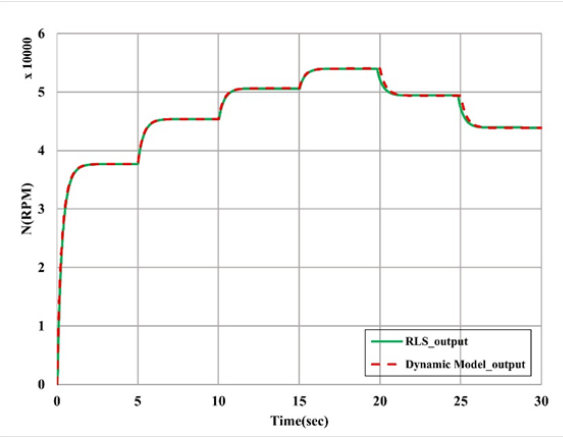

Figure 5- The identified model via RLS is compared with the dynamic model of the engine at the design point.

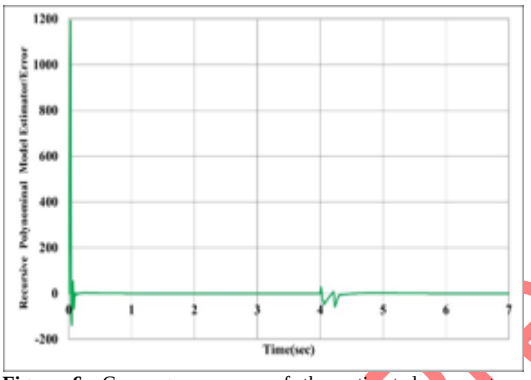

Figure 6- Convergence error of the estimated parameters by recursive polynomial model estimator.

Therefore, more errors are created at these points in the computation process. One familiar and good solution to this problem is segmenting the functional curve based on β lines. The value of β in the cross of the choke line and the surge line equals zero and one, respectively. By the way, the values of β are only mathematical planes and don't have any physical concept. The performance curves are included inside the nonlinear model as two-dimensional tables consisting of β, efficiency, corrected speed, and air mass flow. Owing to the β-lines with the pressure ratio lines being parallel, the values of the β lines are calculated only via equation (18). A constrained MPC controller was designed for the engine. Then, the system's functional purposes with the controller were investigated according to the defined parameters in Table ٢. For this reason, first, the nonlinear model was linearized via the adaptive technique based on the recursive least squares estimator and ARX structure at the design point. The model was applied to the MPC controller as a linear internal model. The controller design process is as follows: The generated control signal by the MPC controller and the rotor speed system are applied to the RLS estimator as the input. The estimator estimates the fifth-order linear model parameters based on the ARX structure, which is suitable for any operating point. The linear model is rewritten in augmented form to reduce the output steady-state error. Finally, the MPC controller coefficients are calculated and applied to the Hildreth algorithm for control command generation. The control objective is that the system output tracks the desired rotor speed (as an indication of thrust because the thrust is an unmeasurable variable) and, to protect the permissible bounds of physical constraints simultaneously.

The simulation results indicate that the proposed controller, without exceeding limits (limit protection) and without the switching in controller/model, can track the pilot's request (power management) at all. Operating points of the engine flight envelope (the limit values are described in Table 3). Three shaft speed control scenarios are applied to the system. Simulations under two flight conditions existing in the engine flight envelope are carried out, and the MPC controller performance is compared with the Min/PID structure. The results of evaluating the performance of both controllers against the engine dynamics variation due to the flight conditions (Mach numbers and altitude) variations in the presence of constraints are illustrated in the figures (14-22). Research and industrial experiences show that the PI/PID is a powerful controller. The main challenge of this controller is that it is a linear controller and can only work well in the neighborhood of the linearized operating point. The gain schedule controller also needs piecewise linear models, and to cover the engine flight envelope, switching between one gain and another gain is required. However, the proposed controller in this study can solve this challenge without retuning and switching.

As mentioned, four scenarios are carried out in MATLAB to investigate the designed controller performance, which are explained below. In the first scenario, the simulation is implemented at Mach 0, altitude 0 m, and 100% engine speed without any constraint on the turbine exhaust temperature and control input.

This scenario carries an acceleration from 70% engine speed to 100% of the engine speed (57000 rpm) as the step input without any constraints. In Figure 7, the performance of the MPC controller is compared the PID controller (shaft speed N). As expected, speed tracking is performed satisfactorily, and both controllers work well. The first scenario in another operating point (Mach 0.8 and altitude of 8000 m) is repeated, while the rest of the conditions remain invariant in the controller and model (figures 8-9).

As can be seen, despite the change in environmental conditions, both controllers will still perform well. The results at the new operating point show that at the acceleration time of the fourth second, the system's output with the PID controller follows the set point with a rise time of about 0.068. While the system with the MPC controller follows the set point without overshoot, there is an increase in the rise time (about 0.125 seconds).

Figures (10-11) describe the engine performance under the second scenario at Mach 0 and altitude 0 m. In this scenario, successive acceleration up to 100% engine speed and then deceleration over 30 seconds, without limit protection, is implemented. As can be seen, the PID controller, despite having damped fluctuations during acceleration and deceleration moments, can still track the set point, while the MPC controller tracks the set point without fluctuations in the transient and steady state of the scenario.

Therefore, both controllers still have acceptable performance at different power settings in this operating point. To check the effects of variations in environmental conditions and operating point variations on system performance, the second scenario was repeated at another flight condition (altitude 8000 and Mach number 0.8). The response of the speed and exhaust temperature in this process is depicted in Figs. 12-13. The simulation result shows that the change in operation point does not affect the engine performance, and the tracking is performed well.

The engine response with the PID controller during the acceleration and deceleration has small fluctuations, but is still acceptable. It may be possible to adjust the PID controller

In Press, Pre-Proof Version

coefficients better by investigating the experimental data more precisely, so that it prevents fluctuations in the system response.

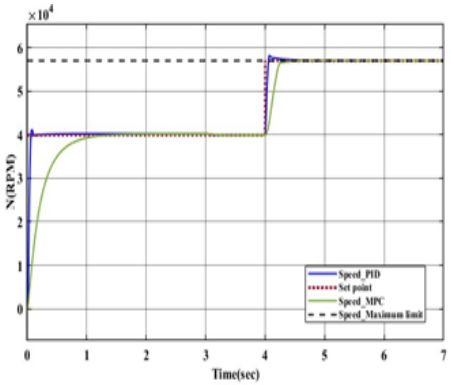

Figure 7- Scenario1.Comparison of the shaft speed response of two controllers to the step set-point without limit protection at Mach number 0 and altitude 0 m.

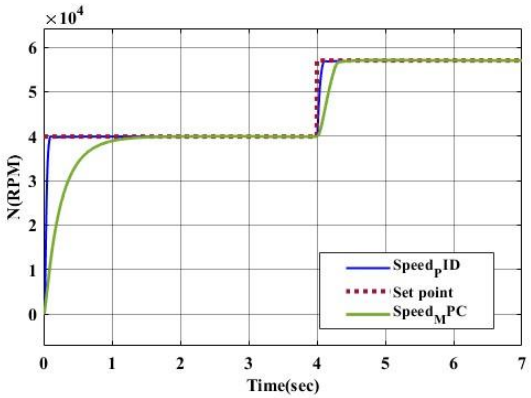

Figure 8- Scenario 1b. Comparison of the shaft speed response of two controllers to the step set-point without limit protection at Mach number 0.8 and altitude 8000 m.

Considering that, the best efficiency and high performance for aero engines will be obtained near the limitations. Fuel mass flow is a vital variable in the engine for two reasons: 1. from an economic point of view, and 2. the protection of the engine. The extra injection of the fuel may cause dangerous events.

Therefore, it is necessary to consider a limit on the control input. The next challenge in the design process is to simultaneously provide the desired thrust at different operating points with limit protection. The third scenario, in two steps, was implemented for this purpose. This scenario was accomplished in the presence of the turbine outlet temperature limit and control input limit at two different flight conditions. The figures (14-19) describe the simulation results at the two operating points. This time, both acceleration and deceleration processes are performed in the presence of limits. The turbine exhaust temperature signal at the first operating point is shown in Fig.15. The MPC controller tracks the set point correctly, accepting a percentage of the error in the presence of all the constraints. In contrast, the PID controller performs the tracking with more error.

The temperature and control input are maintained below the maximum level at this operating point (Figures 15-16). The second step of this scenario is carried out at Mach 0.8 and an altitude of 8000m.The simulation results of this stage are presented in Figs. (17- 19). At the 15th second, when the maximum speed is requested, the PID controller cannot protect the maximum value of the turbine outlet temperature and fuel flow rate, and tracking is also not lost. After 5 seconds, the integrator reduced the error, and the output tracked the command. While the MPC controller reliably tracks the reference while maintaining the constraints. The findings indicate that the proposed controller can address the main challenges, including power management in the whole flight envelope and limit protection in the aero engine control system design process.

Also, it can maintain the performance criteria across all the power settings to provide a quick and appropriate response. To provide a more precise comparison with the existing method, the transient state characteristics (rising time, settling time, overshoot percentage) and steady state (control error) of the constrained control system (in the presence of temperature constraint), under the fourth scenario, are proposed. A step input from 70% to 87% of the final engine speed was applied to the system (Figures 20-22).

As shown in Figure 20, the system controlled by the PID controller with a settling time of 1.857 seconds, a rise time of 0.364 seconds, an overshoot value of 27.7 %, and a steady-state error of 0.2% tracks the reference input. Meanwhile, the predictive controller, without overshooting, tracks the input with a rise time of about 0.812 and a steady-state error of zero. The results show that the predictive controller tracks the reference input at a slower speed than the controller PID, but without overshoot and steady state error. To check the turbine temperature (T5) limit adherence rates, the system was tested in the presence of a temperature constraint under different operating conditions, without changing or adjusting any control parameters (Figure 21). As it is clear, the predictive controller has tracked the reference input well under various environmental conditions while maintaining the turbine temperature constraint (the maximum temperature from minimum altitude and Mach to maximum altitude and Mach is varying from 541 ($°k$) up to 645($°k$). In contrast, the PID controller cannot protect the turbine temperature, and with flight condition variations, it exceeds the maximum limit.

6-Conclusion

This research aims to design a fuel flow control system based on a novel MPC control technique for aero engines. The design process uses an adaptive method to calculate the model coefficients in each new operation condition. The results of the first scenario showed that in the absence of constraints, both controls perform well under different operating conditions. It may even be possible that the PI controller may have a better response. Using a gain schedule control or designing an individual PID/PI controller for each operating point may be a good solution for covering the whole of the flight envelope. But these techniques need to be retuned for new operating range, possibly leading to the switching problem. In addition, considering the effect of environmental conditions and providing the proper response to different power settings in quick maneuvers will be hard in such controllers. For this reason, in the second scenario, an acceleration process and then a deceleration were considered to investigate this subject. Of course, this scenario was done without limitations, and the controller coefficients remained unchanged. The second test findings indicated that both controllers can track the set point, but the MPC controller performs better than the PID controller in transient mode. The effects of flight conditions variations on aero-engine performance in the presence of the limits were studied in two steps in the third scenario. The results of the first step of this test revealed that the MPC controller managed the temperature limit and tracked the set

In Press, Not Proof Version

point well, of course, with accepting the percentage of the error. Meanwhile, the PI controller lost tracking when the temperature reached its maximum limit.

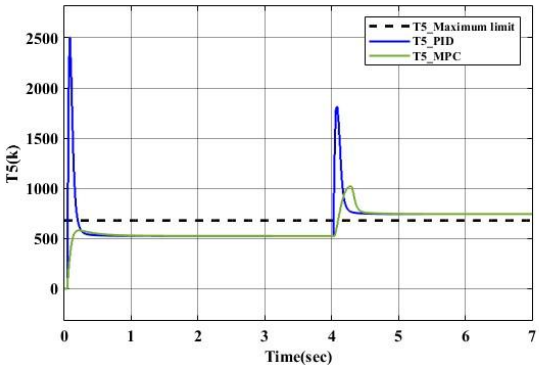

Figure 9- Scenario 1b. Comparison of the turbine exhaust temperature response of two controllers at the Mach number 0.8 and altitude 8000 m.

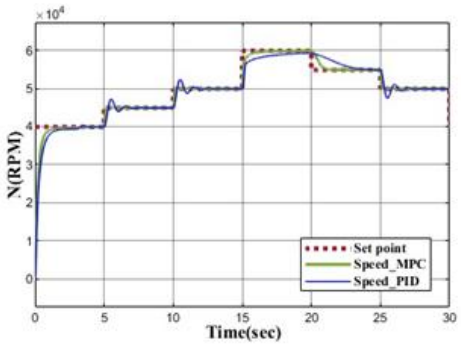

Figure 10- Scenario2. Comparison of the shaft speed response of two controllers at Mach number 0 and altitude 0 m.

In the second step, a control input limit was also added to both systems. The test results indicate that the MPC controller maintains the temperature under the maximum level while quickly responding to all pilot requests with minimum overshoot. The findings and results prove that the proposed controller can provide the required response in different power settings. It can also keep critical variables within the permitted bounds, without retuning the controller when the operating condition varies. However, the PID controller at some operation points exceeds the permission level and loses tracking at the maximum shaft speed.

Artificial Intelligence Statement: No artificial intelligence tools were used in the preparation of this research.

Funding: This research has not received any specific grants from funding agencies in the public, commercial, or non-profit sectors.

Authorship Contribution: All authors contribute equally.

Conflict of Interest: All the authors have no conflicts of interest.

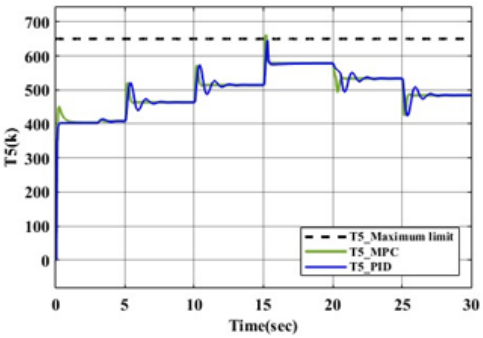

Figure 11- Scenario2. Comparison of the T5 response of two controllers at Mach number 0 and an altitude of 0

In Press - Proof

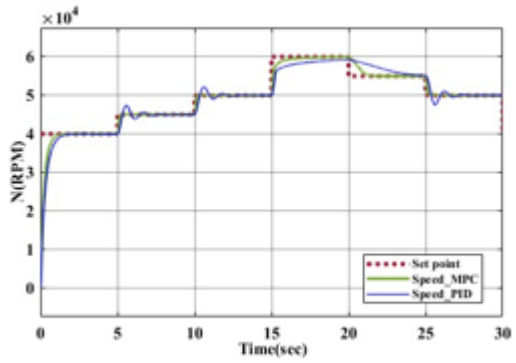

Figure 12- Scenario2b. Comparison of the shaft speed response of two controllers at the Mach number of 0.8 and altitude 8000 m.

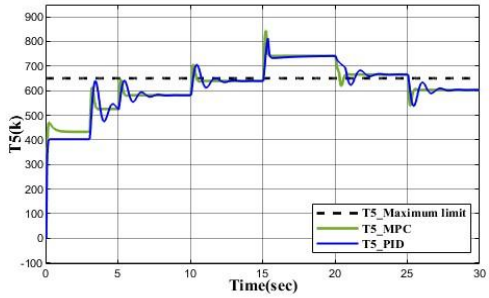

Figure 13-. Scenario2b. Comparison of the turbine exhaust temperature at the Mach number of 0.8 and altitude 8000 m.

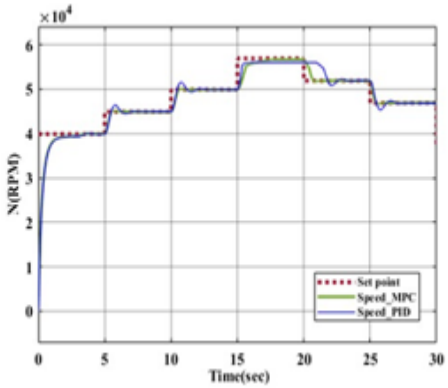

Figure 14- Scenario3. Shaft speed at a Mach number 0 and altitude 0 m.

In Press, Pre-Proof Version

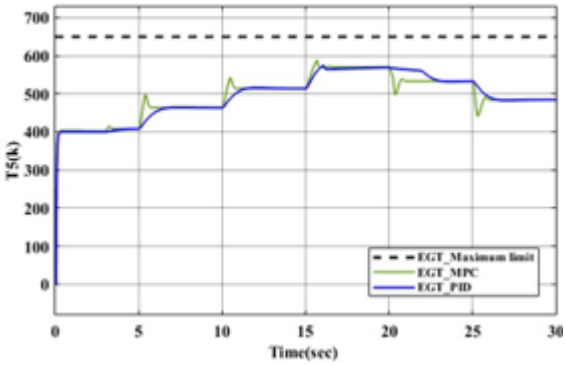

Figure 15- Scenario3. T5 response at a Mach number 0 and altitude 0 m.

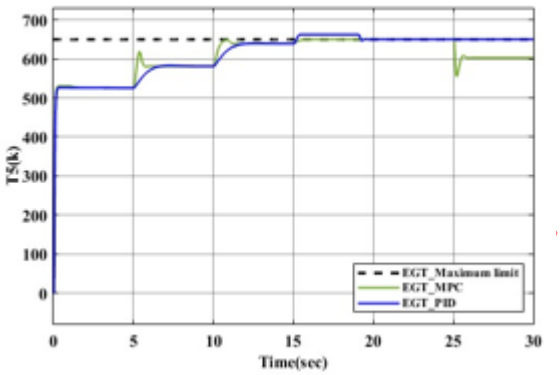

Figure 18- Scenario3b. Comparison of T_5 response at the Mach number of 0.8 and an altitude of 8000 (m).

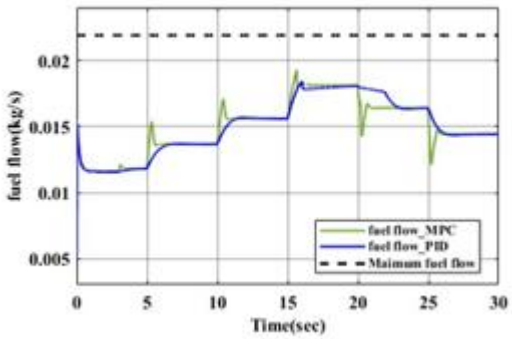

Figure 16- Scenario3. The calculated fuel flows by both controllers in the presence of limits at Mach number ・ and altitude m.

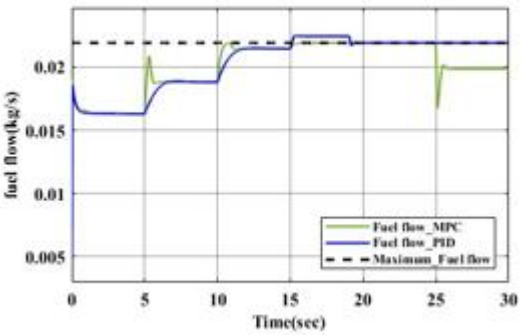

Figure 19- Scenario3b. The calculated fuel flows by both controllers in the presence of limits at a Mach number of 0.8 and altitude of 8000 m.

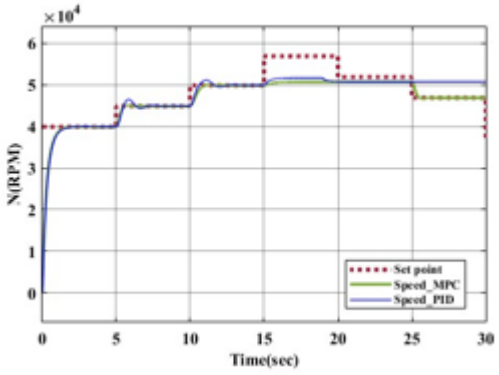

Figure 17- Scenario3b. Comparison of the shaft speed response of two controllers at Mach number of 0.8 and an altitude of 8000 m.

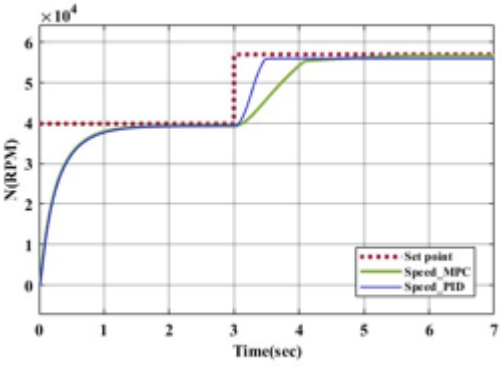

Figure 20- Scenario4. Shaft speed response at a Mach number of 0 and altitude 0 m.

Pre-Proof

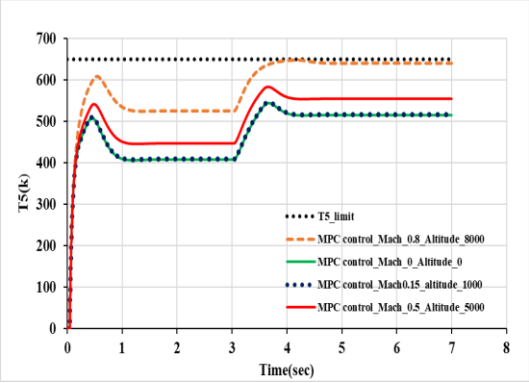

Figure 21-Scenario4. Investigating the effect of the operation condition on the turbine temperature limit adherence in the presence of the MPC controller.

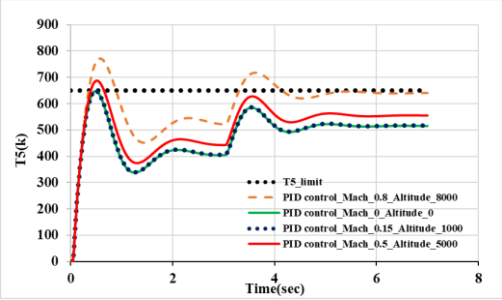

Figure 22- Scenario4b. Investigating the effect of operation conditions on the turbine temperature limit adherence in the presence of the PID controller.

Table 3- Maximum limit of the engine variables

Number	Variable name	Value
1	Maximum value of shaft speed (rpm)	57000
2	Maximum turbine exhaust temperature (°K)	680
3	Maximum input control (fuel mass flow rate) (kg/s)	530

Nomenclature

A_N	the effective cross-sectional area of the nozzle (m^2)
A_{cons}	Vector of system constraints
A, B, C	State-space matrices of the system
a_i, b_i	Model parameters
b	Constrained variables
Bld	compressor bleed flow rate (kg/s)
C_v	specific constant at constant volume (J/(kg. k))
C_{v4}	Specific constant at constant volume at the combustor interpolated temperature((J/(kg.k)))
C_p	specific heat capacity in constant pressure (J/kg.k)
C_{p4}	specific constant at constant pressure at the combustor interpolated temperature (J/kg.k)
d_{ij}	ij-th element of the matrix 'd'
$e(k)$	Error vector
f_1	lookup table (Function for the corrected mass flow rate of the compressor as the compressor map)
f_2	lookup table (Function for the corrected mass flow rate of the turbine as the turbine map)
g_1	lookup table (Function for the isentropic efficiency of the compressor as the compressor map)
g_2	lookup table (Function for the isentropic expansion efficiency of the turbine as the turbine map)
I	moment of inertia of shaft (kg.m^2)
J	Controller cost function
k	time step
k_i	the i-th element of the matrix 'K'
LHV	The calorific value of fuel (J/kg)
M	Mach number
$\dot{m}_{c,comp}$	Compressor-corrected mass flow rate
$\dot{m}_{3in}$	mass flow rate at the entrance of the compressor plenum (kg/s)
$\dot{m}_{3out}$	mass flow rate at the exit of the compressor plenum (kg/s)
$\dot{m}_{fuel}$	the mass flow rate of the fuel (kg/s)
$\dot{m}_{4in}$	the mass flow rate in the combustor (kg/s)
$\dot{m}_{4out}$	mass flow rate at the exit of the combustor plenum (kg/s)
$\dot{m}_{5in}$	mass flow rate at the entrance of the turbine plenum(kg/s)
$\dot{m}_{5out}$	mass flow rate at the exit of the turbine plenum (kg/s)
$\dot{m}_6$	mass flow rate at the exit of the nozzle (kg/s)
N_{sh}	shaft speed (RPM)
$N_{c,comp}$	corrected speed for the compressor
$N_{c,turb}$	corrected speed for the turbine
N_{des}	shaft speed at the design point (RPM)
N	Number of samples
n	Order of controlled system
N_c, N_p	control and prediction horizons
P_{amb}	ambient static pressure
P_b	nozzle back pressure

In Press, Pre-Pr

P_{cr}	critical pressure ratio for the nozzle
P_{ref}	reference pressure at sea level = 101324 ($N/m^2 = pa$) =14.696 psi
P_0	ambient total pressure
P_2	total pressure at compressor inlet (Psi)
P_3	total pressure at compressor exit (Psi)
P_4	total pressure at the combustor exit
P_5	total pressure at the turbine exit
P_e	total pressure at the nozzle exit
P_{cal}	calculated combustor pressure loss coefficient
P_{back}	nozzle back pressure (Psi)
pr	Pressure ratio
Pw_{comp}	compressor power (KW)
Pw_{turb}	turbine power (KW)
R	universal gas constant
$r(k_i)$	reference trajectory
r_w	Adjustment parameter for the closed loop desired performance
T_{amb}	ambient static temperature ($°k$)
T_b	interpolated temperature in the combustor (k)
T_{ref}	reference temperature at sea leve =288.15 (k)
T_0	ambient total temperature
T_2	total temperature at compressor inlet (k)
T_{2des}	the total temperature at the compressor inlet at the design point ($°k$)
T_{3in}	the total temperature at the compressor inlet plenum ($°k$)
T_{3out}	the total temperature at compressor plenum exit (k)
T_4	the total temperature at the combustor exit
$T_{4,des}$	the total temperature at the combustor exit at the design point
T_{5in}	the total temperature at the turbine plenum inlet
T_{5out}	the total temperature at the turbine plenum exit
T_s	Simulation sample time
u(k)	vector of control variables
u_{min}, u_{max}	vector of lower and upper bounds of the inputs
V	Least Square cost function
V_3	compressor volume (m^3)
V_4	combustor volume (m^3)
V_5	turbine volume (m^3)
W_3	mass of the air in the compressor (kg)
W_4	mass of the air in the combustor(kg)
W_5	mass of the air in the turbine(kg)
$x(k_i)$	vector of state variables (it gives the current information of the system)
y(k)	vector of measured output variables
$y_u(k)$	vector of model output variables
$\hat{y}(k)$	vector of predicted outputs
y_{min}, y_{max}	vector of lower and upper bounds of the outputs
ΔP	pressure loss
β	hypothetical lines
β_b	temperature interpolation constant in the combustor
γ	the ratio of specific heats
γ_b	The ratio of specific heat at the combustor interpolated temperature.
η_{burn}	combustor efficiency
η_I	inlet efficiency
η_{comp}	isentropic compression efficiency in the compressor
η_{turb}	Isentropic expansion efficiency in the turbine
θ	Model parameters vector
λ	Lagrange coefficient
μ	Correction vector
Ψ	Data vector
Subscripts	
a	augmented matrix
amb	ambient
burn	burner
c	corrected
comp	compressor
d	discrete-time
out	outlet
e	exit
in	inlet
N	nozzle
out	outlet
turb	turbine
Superscript	
T	transpose

References

[1] X. Zhou, F. Lu, W. Zhou, and J. Huang, "An improved multivariable generalized predictive control algorithm for direct performance control of gas turbine engine," *Aerospace Science and Technology*, vol. 99, p. 105576, 2020.

[2] E. B. E. Saleh and A. Gawad, "Modeling and simulation of a double spool turbofan engine using simulink®," *Ph. D. thesis*, 2017.

[3] M. Montazeri-Gh, A. Rasti, A. Jafari, and M. Ehteshami, "Design and implementation of MPC for turbofan engine control system," *Aerospace Science and Technology*, vol. 92, pp. 99-113, 2019.

[4] R. D. May and S. Garg, *Reducing conservatism in aircraft engine response using conditionally active min-max limit regulators*. American Society of Mechanical Engineers, 2012.

[5] F. W. Burcham Jr, C. G. Fullerton, and T. A. Maine, "Manual manipulation of engine throttles for emergency flight control," 2004.

[6] A. Imani and M. Montazeri-Gh, "A Min–Max multiregulator system with stability analysis for aeroengine propulsion control," *ISA transactions*, vol. 85, pp. 84-96, 2019.

[7] H. Asgari, X. Chen, and R. Sainudiin, "Modelling and simulation of gas turbines," *International Journal of Modelling, Identification and Control*, vol. 20, no. 3, pp. 253-270, 2013.

[8] C. Kong and J. Park, "Transient performance simulation of propulsion system for CRW type UAV using SIMULINK," in *Proc. 24th Int. Congr. Aeronaut. Sci.*, 2013, pp. 1-8.

[9] N. Rahman and J. F. Whidborne, "A numerical investigation into the effect of engine bleed on performance of a single-spool turbojet engine," *Proceedings of the Institution of Mechanical Engineers, Part G: Journal of Aerospace Engineering*, vol. 222, no. 7, pp. 939-949, 2008.

[10] S. Martin, I. Wallace, and D. G. Bates, "Development and validation of an aero-engine simulation model for advanced controller design," in *2008 American Control Conference*, 2008: IEEE, pp. 2334-2339.

[11] S. Martin, "Development and validation of a civil aircraft engine simulation model for advanced controller design," University of Leicester, 2010.

[12] M. Kulyk, I. Lastivka, L. Volianska, A. Voznyuk, and I. Babichev, "Mathematical Modeling of Operating Process Parameters of a Mixed-flow Turbofan Engine with an Afterburner," *Journal of Aerospace Technology and Management*, vol. 16, p. e2824, 2024.

[13] J. R. Szuch, J. F. Soeder, K. Seldner, and D. S. Cwynar, "F100 multivariable control synthesis program: Evaluation of a multivariable control using a real-time engine simulation," 1977.

[14] J. F. Soeder, "F100 Multivariable Control Synthesis Program. Computer Implementation of the F100 Multivariable Control Algorithm," 1983.

[15] Y. Zhu, M. Pan, W. Zhou, and J. Huang, "Intelligent direct thrust control for multivariable turbofan engine based on reinforcement and deep learning methods," *Aerospace Science and Technology*, vol. 131, p. 107972, 2022.

[16] Y. Qi, W. Bao, and J. Chang, "State-based switching control strategy with application to aeroengine safety protection," *Journal of Aerospace Engineering*, vol. 28, no. 3, p. 04014076, 2015.

[17] H. Richter, "Multiple sliding modes with override logic: Limit management in aircraft engine controls," *Journal of guidance, control, and dynamics*, vol. 35, no. 4, pp. 1132-1142, 2012.

[18] W. Gao, X. Zhou, M. Pan, W. Zhou, F. Lu, and J. Huang, "Acceleration control strategy for aero-engines based on model-free deep reinforcement learning method," *Aerospace Science and Technology*, vol. 120, p. 107248, 2022.

[19] D. Ring and M. Henriksson, "Thrust control for a turbofan engine using estimation," in *Turbo Expo: Power for Land, Sea, and Air*, 2006, vol. 42371, pp. 901-910.

[20] S. Chatterjee and J. Litt, "Online model parameter estimation of jet engine degradation for autonomous propulsion control," in *AIAA Guidance, Navigation, and Control Conference and Exhibit*, 2003, p. 5425.

[21] A. Kreiner and K. Lietzau, "The use of onboard real-time models for jet engine control," *MTU Aero Engines*, 2003.

[22] S. Jafari and T. Nikolaidis, "Turbojet engine industrial Min–Max controller performance improvement using fuzzy norms," *Electronics*, vol. 7, no. 11, p. 314, 2018.

[23] A. Imani and M. Montazeri-Gh, "A Min-Max selector controller for turbofan engines with improvement of limit management and low computational burden," *Transactions of the Institute of Measurement and Control*, vol. 41, no. 1, pp. 36-44, 2019.

[24] P. Shuwei, S. Jafari, T. Nikolaidis, and L. Qiuhong, "Reduced-dimensional MPC controller for direct thrust control," *Chinese Journal of Aeronautics*, vol. 35, no. 4, pp. 66-81, 2022.

[25] S. Pang, Q. Li, and B. Ni, "Improved nonlinear MPC for aircraft gas turbine engine based on semi-alternative optimization strategy," *Aerospace Science and Technology*, vol. 118, p. 106983, 2021.

[26] X. Liu, J. Shi, Y. Qi, and Y. Yuan, "Design for aircraft engine multi-objective controllers with switching characteristics," *Chinese Journal of Aeronautics*, vol. 27, no. 5, pp. 1097-1110, 2014.

[27] Y. Shi and X.-M. Sun, "Bumpless transfer control for switched linear systems and its application to aero-engines," IEEE Transactions on Circuits and Systems I: Regular Papers, vol. 68, no. 5, pp. 2171-2182, 2021.

[28] ا. دوائی- مرکزی، "طراحی رویکرد کنترلی مبتنی بر یادگیری تقویتی و روش تطبیقی -فازی-لغزشی جهت کنترل سیستم‌های سوئیچینگ،" مهندسی مکانیک مدرس, vol. 25, no. 2, pp. 87-95, 2025, doi: 10.48311/mme.25.2.87. and ح. صفری، ا. خان میرزا

[29] X. Wenhao, J. Huang, Q. Jiakun, and P. Muxuan, "Limit protection design in turbofan engine acceleration control based on scheduling command governor," *Chinese Journal of Aeronautics*, vol. 34, no. 10, pp. 67-80, 2021.

[30] س. شجاعی، "کنترل یکپارچه طولی و عرضی برای ردیابی مسیر خودروی خودران مبتنی بر کنترل‌کننده پیش‌بین مدل غیرخطی و تخمین‌گر افق لغزان در شرایط تاخیر و عدم قطعیت شبکه،" مهندسی مکانیک مدرس, vol. 26, no. 7, pp. 583-597, 2026, doi: 10.48311/mme.2026.118574.82920. and ش. آزادی

[31] J. Nayler, "Gas Turbine Theory, Rogers Cohen and Saravanamuttoo, Longman Group Ltd. 1972. 337pp. Illustrated.£ 5.95 net (paperback):£ 7.95 (cased)," *The Aeronautical Journal*, vol. 77, no. 748, pp. 195-196, 1973.

[32] S. Yarlagadda, "Performance analysis of J85 turbojet engine matching thrust with reduced inlet pressure to the compressor," University of Toledo, 2010.

[33] S.-T. Lin, J.-H. Lu, M.-C. Hong, and K.-W. Hsu, "Real-Time Dynamic Simulation of Single Spool Turboj et Engines," *Simulation*, vol. 73, no. 6, pp. 352-361, 1999.

[34] P. P. Walsh and P. Fletcher, *Gas turbine performance*. John Wiley & Sons, 2004.

[35] L. Wang, *Model predictive control system design and implementation using MATLAB*. Springer, 2009.

[36] K. J. Astrom, "Adaptive feedback control," *Proceedings of the IEEE*, vol. 75, no. 2, pp. 185-217, 1987.

In Press Pre-Proof Version

In Press, Pre-Proof Version